

1

1 **Reliability of recharge rates estimated from groundwater**

2 **age with a simplified analytical approach**

3

4

5

6 Yanhui Dong^{1,2,3}, Yueqing Xie^{4,5}, Jun Zhang^{6,*}, Andrew J. Love⁵, Xin Dai⁴

7

8 ¹ Key Laboratory of Shale Gas and Geoengineering, Institute of Geology and

9 Geophysics, Chinese Academy of Sciences, Beijing 100029, China

10 ² College of Earth and Planetary Sciences, University of Chinese Academy of

11 Sciences, Beijing 100049, China

12 ³ Innovation Academy for Earth Science, Chinese Academy of Sciences, Beijing,

13 100029, China

14 ⁴ Ministry of Education Key Laboratory of Surficial Geochemistry, School of Earth

15 Sciences and Engineering, Nanjing University, Nanjing, China

16 ⁵ National Centre for Groundwater Research and Training, College of Science &

17 Engineering, Flinders University, Adelaide 5001, Australia

18 ⁶ Key Laboratory for Groundwater and Ecology in Arid and Semi-Arid Areas, Xi'an

19 Center of Geological Survey, CGS, Xi'an, China

20 * Corresponding author: Jun Zhang, zhangjun1982@qq.com

21

24 **Abstract**

25 Groundwater age is often used to estimate groundwater recharge through a simplified
26 analytical approach. This estimated recharge is thought to be representative of the
27 mean recharge between the point of entry and the sampling point. However, given the
28 complexity in actual recharge, whether the mean recharge is reasonable is still
29 unclear. This study examined the validity of the method to estimate long-term average
30 groundwater recharge and the possibility of obtaining reasonable spatial recharge
31 pattern. We first validated our model in producing reasonable age distributions using a
32 constant flux boundary condition. We then generated different flow fields and age
33 patterns by using various spatially-varying flux boundary conditions with different
34 magnitudes and wavelengths. Groundwater recharge was estimated and analyzed
35 afterwards using the method at the spatial scale. We illustrated the main findings with
36 a field example in the end. Our results suggest that we can estimate long-term average
37 groundwater recharge with 10% error in many parts of an aquifer. The size of these
38 areas decreases with the increase in both the amplitude and the wavelength. The
39 chance of obtaining a reasonable groundwater recharge is higher if an age sample is
40 collected from the middle of an aquifer and at downstream areas. Our study also
41 indicates that the method can also be used to estimate local groundwater recharge if
42 age samples are collected close to the water table. However, care must be taken to

43 determine groundwater age regardless of conditions.

44

45 Key words: simplified analytical approach; groundwater age; spatial groundwater
46 recharge

47 **1. Introduction**

48 Groundwater recharge is defined as water reaching water table to replenish an aquifer.

49 It occurs in a number of forms including diffuse recharge, focused recharge and

50 artificial recharge and is an important component of a groundwater water balance (de

51 Vries & Simmers, 2002). Recharge rates are critical for determining sustainable

52 groundwater extraction rates, properly understanding groundwater flow and storage

53 and reducing uncertainty in groundwater numerical models. A variety of methods

54 have been developed to estimate groundwater recharge, such as soil water balance,

55 water table fluctuation and age tracer methods (Allison, Gee, & Tyler, 1994; Healy,

56 2010; Scanlon, Healy, & Cook, 2002). The age tracer method is often used in recharge

57 estimation because groundwater age usually integrates flow information across large

58 areas and over long periods (Cook & Böhlke, 2000).

59

60 The use of age tracers to estimate groundwater recharge needs to rely on a simplified

61 analytical method, introduced by Vogel (1967). The equation is given by

$$62 \quad R_V = \frac{H\theta}{t} \ln \left(\frac{H}{H-h} \right) \quad (1)$$

63 where R_V is the Vogel-based recharge [$L T^{-1}$], t is the time since recharge at a point in

64 the aquifer [T], θ is the porosity [-], H and h are the aquifer thickness [L] and the

65 vertical distance between the point of sampling and the land surface [L], respectively.

66 This method is based on several assumptions including horizontal flow, uniform
67 recharge, homogeneous aquifer material and negligible dispersion effect. The relevant
68 conceptualization is shown in Figure 1. Because this method requires very few
69 parameters compared to some other analytical equations (Chesnaux, Molson, &
70 Chapuis, 2005; Chesnaux, Santoni, Garel, & Huneau, 2018), it has been widely used
71 in many different conditions despite assumptions made (Hinkle, Böhlke, Duff,
72 Morgan, & Weick, 2007; Harrington, Cook, & Herczeg, 2002; Hagedorn, El-Kadi,
73 Mair, Whittier, & Ha, 2011; Kozuskanich, Simmons, & Cook, 2014; McMahon,
74 Plummer, Böhlke, Shapiro, & Hinkle, 2011). For example, Hagedorn, El-Kadi, Mair,
75 Whittier, & Ha (2011) used this method to estimate recharge in a fractured aquifer on
76 the Jeju Island by assuming that groundwater flow in fractures and porous media are
77 equivalent. Hinkle, Böhlke, Duff, Morgan, & Weick (2007) estimated large-scale
78 recharge with this method in order to examine distribution of nitrate and ammonium
79 in groundwater.

80

81 Compared to the assumption of this analytical method, actual groundwater recharge is
82 known to vary in space because of spatial distributions of controlling factors including
83 climate, soil and vegetation (Cook & Böhlke, 2000; Cook, Walk, & Jolly, 1989; Kim
84 & Jackson, 2012; Keese, Scanlon, & Reedy, 2005; Scanlon et al., 2006; Xie, Crosbie,
85 Simmons, Cook, & Zhang, 2019; Xie, Crosbie, Yang, Wu, & Wang, 2018). It is
86 evident that different spatial patterns in recharge may result in different flow fields
87 which lead to different groundwater age patterns. Hence, groundwater recharge

88 estimated from the Vogel method would differ from location to location. Whether and
89 under what conditions this simplified analytical method still produces representative
90 long-term average estimates is still unclear.

91

92 Spatially varying groundwater recharge is one of several important factors in
93 determining groundwater flow fields (Sanford, 2002). Estimating spatial groundwater
94 recharge has been difficult. Therefore, many studies usually use a limited number of
95 estimates to represent large areas (e.g., Xie, Cook, Shanafield, Simmons, & Zheng,
96 2016; Yang et al., 2019). Groundwater tracers underneath water table result mostly
97 from local recharge and so groundwater age must vary spatially (McMahon, Bohlke,
98 & Carney, 2007). It is likely that the analytical method could also estimate spatial
99 recharge and infer water table behavior by examining groundwater age at shallow
100 parts of aquifers (McMahon, Bohlke, & Carney, 2007; Wood, Cook, & Harrington,
101 2015). However, as the Vogel method was developed based on several assumptions,
102 whether it can yield reasonable results warrants careful assessment.

103

104 This study attempted to examine whether the Vogel method is capable of estimating
105 long-term average groundwater recharge and the possibility of estimating spatially-
106 varying groundwater recharge with such a method. We first established a groundwater
107 flow and age transport model with a constant recharge rate along the top boundary
108 and examined it by comparing groundwater age distribution to that calculated with the
109 analytical method. Afterwards, we changed constant groundwater recharge to different

110 spatially-varying recharge that varies in different sinusoidal patterns. The simulated
 111 groundwater age in the model was used to estimate recharge with the analytical
 112 method. The estimated recharge was then compared to the actual recharge to shed
 113 light on the feasibility of the Vogel method for estimating recharge under spatially
 114 changing conditions. A field example was employed in the end to illustrate how our
 115 theoretical analysis could assist in the interpretation of real-world data.

116

117 **2. Methods**

118 **2.1 Governing equations**

119 Several numerical experiments were performed to investigate groundwater age
 120 distribution and examine the validity of the simple method to estimate groundwater
 121 recharge. To simulate groundwater flow and age transport simultaneously, the
 122 numerical code HydroGeoSphere (Aquanty Inc., 2018) was selected.
 123 HydroGeoSphere uses the 3-D Richards equation to simulate variably saturated
 124 groundwater flow. As our system is fully saturated, the equation can be simplified into
 125 the follow form:

$$126 \quad S_s \frac{\partial \psi}{\partial t} = -\nabla \cdot \mathbf{q} + Q \quad (2)$$

127 Where S_s is the specific storage [L^{-1}], Q is the source and sink [T^{-1}], \mathbf{q} is the Darcy flux
 128 tensor [$L T^{-1}$], ψ is the pressure head [L]. \mathbf{q} is given by

$$129 \quad \mathbf{q} = -\mathbf{K} \cdot \nabla(\psi + z) \quad (3)$$

130 where \mathbf{K} is the hydraulic conductivity tensor [$L T^{-1}$] and z is the elevation head [L].

131

132 Groundwater age transport was simulated with the mean age approach (Goode, 1996).
 133 As a groundwater sample contains a large number of water particles, mean age is
 134 usually used in analyses. It is reasonable to assume that the mean age of mixed water
 135 particles is a volume-weighted average if density is constant, and so the mean age will
 136 vary in a similar fashion to the concentration of a conservative solute. Hence, mean
 137 age transport can be described by a variant of the advection-dispersion equation. The
 138 governing equation is given by

$$139 \quad \frac{\partial(\phi A)}{\partial t} = -\nabla \cdot A q + \nabla \cdot (D \cdot \nabla A) + \phi + Q_A \quad (4)$$

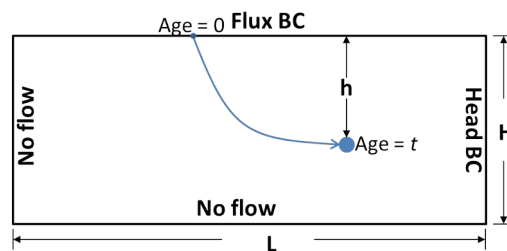
140 where A is the mean groundwater age [T], ϕ is the porosity [-], \mathbf{D} is the hydrodynamic
 141 dispersion tensor [L] and Q_A is the source/sink term of the age mass [-]. The first two
 142 terms on the right-hand side of the equation describe advective and dispersive
 143 transport of age mass, respectively. The third term is age increase at the rate of 1 year
 144 per year along flow paths. The last term represents the exchange of age mass with
 145 other domains. The reader is referred to Aquanty Inc. (2018) for a detailed description
 146 of numerical implementation.

147

148 **2.2 Model setup**

149 The numerical model employed is rectangular in shape (10,000 m in length and 100 m
 150 in thickness) as shown in Figure 1. Kozuskanich, Simmons, & Cook (2014) examined
 151 the effect of aquifer heterogeneity on the applicability of the Vogel method with the
 152 same model setup but smaller size. The model was used to perform groundwater flow
 153 and mean groundwater age transport simulations. For the groundwater flow

154 simulation, a flux boundary condition was applied to the top surface to represent
 155 actual groundwater recharge. A constant rate of 100 mm/y was used in this study. A
 156 head boundary condition of 100 m was specified to the right-hand side boundary. All
 157 the other sides were given no-flow boundary conditions. It should be noted that this
 158 model represents an unconfined aquifer with the sloping bottom despite the
 159 rectangular shape. For the mean age transport simulation, a mean age of zero was
 160 specified at the top boundary where the actual recharge occurred. The model was
 161 discretized with a grid size of 2 m vertically and 10 m laterally, resulting in a total of
 162 50,000 elements. A porosity θ of 0.3 and a hydraulic conductivity K of 0.8 m/d were
 163 specified to the model. Note that K does not affect modeling results given flux
 164 boundary conditions used. For the flow simulation, the model was simulated in steady
 165 state. For the age transport simulation, the model was run for 10,000 years. If evident
 166 change was observed between the last two time steps, the model was run again for
 167 10,000 years.



168

169 **Figure 1** Schematic diagram of the model used in this study. L and H are 10,000 m
 170 and 100 m, respectively. A constant flux of 100 mm/y was used at the top boundary
 171 and a head of 100 m was specified to the right-hand side boundary. These values were
 172 chosen for demonstrative purposes only. Other values could also be used.

173

174 **2.3 Spatially-varying actual recharge**

175 In order to examine the validity of the Vogel method to estimate groundwater
176 recharge, we generated groundwater flow fields with different spatially-varying actual
177 recharge conditions along the top surface, realized through flux boundary conditions.

178 The spatially-varying actual recharge is given by

$$179 \quad R_m = A \left(\sin \frac{2\pi}{B} x \right) + C \quad (5)$$

180 where R_m is the modelled recharge [$L T^{-1}$], A , B and C represent the amplitude [$L T^{-1}$],
181 the wavelength [L] and the mean recharge [$L T^{-1}$], respectively, x is the distance from
182 the left end of the top surface [L]. R_m is the theoretical recharge as opposed to the
183 estimated recharge with the Vogel method R_V . In order to be consistent with
184 conventional uses, we use millimeters per year for a recharge rate and meters for
185 length.

186

187 Two types of variations in the recharge were used, including changes in the amplitude
188 and changes in the wavelength. Four recharge amplitudes were considered including
189 12.5, 25, 35 and 50 mm/y and six recharge wavelengths were simulated including
190 500, 1000, 1250, 2000, 3500 and 5000 m. C was constant at 100 mm/y for all the
191 scenarios. Figure 2a and Figure 2b demonstrate how R_m varies with A and B spatially,
192 respectively. Apart from the mean recharge of 100 mm/y, we also examined several
193 different mean values, including 150 mm/y, 50 mm/y. The corresponding amplitudes
194 were varied between 10% and 50% of the mean values, and the wavelengths remained

195 unchanged. A total of 72 scenarios were simulated.

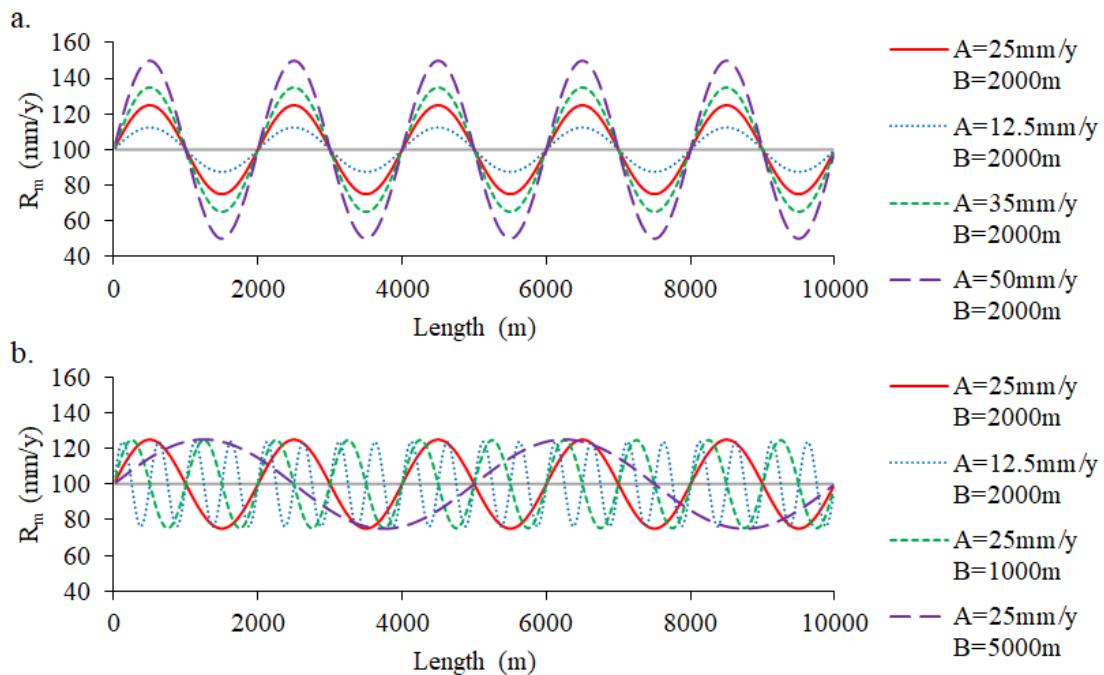
196

197 It should be noted that R_m is dependent on several factors including climate, soil,

198 vegetation, topographic relief. Spatial R_m patterns are difficult to quantify precisely.

199 Despite highly idealized, the R_m patterns used in this study are expected to help

200 improve theoretical understanding of using the Vogel method in complex conditions.



201

202 **Figure 2** Demonstrative sinusoidal variation in modelled groundwater recharge (R_m)

203 with (a) the change in the amplitude A, and (b) the change in the wavelength B.

204

205 3. Results

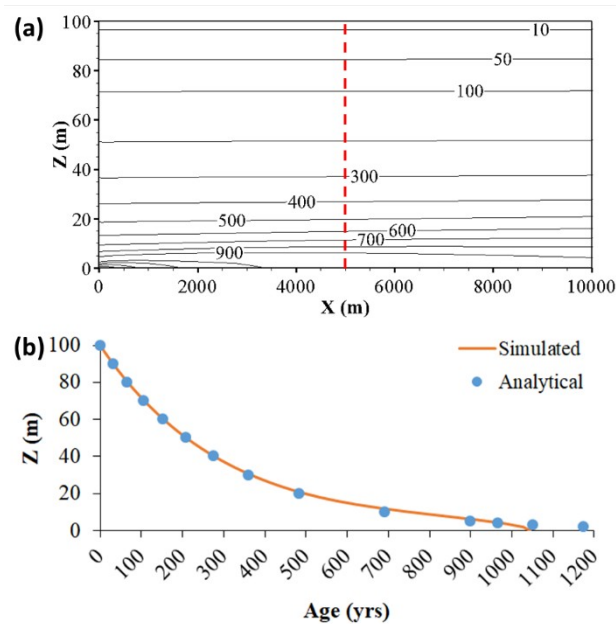
206 3.1 Model validation

207 Model validation was performed by examining the age distribution with constant

208 recharge. The result shows that simulated groundwater age is constant horizontally for

209 most part of the aquifer domain (approximately the range of $Z = 20$ to $Z = 100$ m)
 210 (Figure 3a). Close to the bottom ($Z = 0$ to 10 m), the simulated age was slightly
 211 greater on the left than that on the right due to bottom boundary effect. Figure 3b
 212 shows an excellent match between the simulated and the analytical age profiles at $X =$
 213 5000 m. It can be seen that under ideal conditions the groundwater age increases with
 214 depth exponentially. The comparison suggests that our numerical model closely
 215 matches the analytical solution and therefore can be used to simulate more complex
 216 groundwater flow and age simulations.

217



218

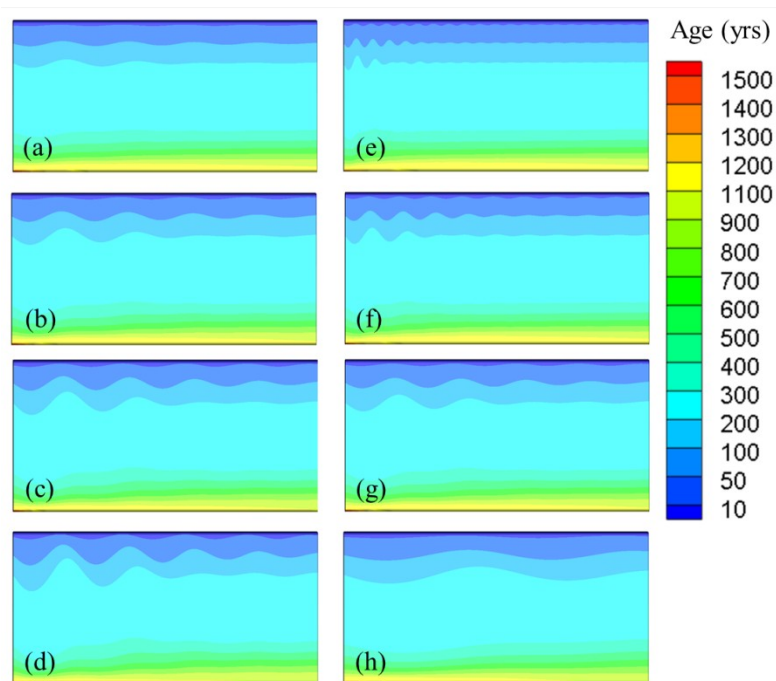
219 **Figure 3** Numerical modeling results: (a) simulated groundwater age distribution with
 220 constant actual groundwater recharge at 100 mm/y for the entire top surface; (b)
 221 comparison of simulated to analytical groundwater age profiles at 5000 m as indicated
 222 with a red dashed line in (a). The analytical groundwater age was calculated by
 223 rearranging Equation (1) to obtain t .

224

225 3.2 Spatial distributions in simulated age and estimated recharge

226 We first simulated groundwater age with a specific R_m recharge case along the top
 227 surface ($A = 25$ mm/y and $B = 2000$ m, red solid curves in Figure 2). The spatial
 228 variation in the specific R_m causes groundwater age to vary with depth and also with
 229 distance further downgradient (Figure 4b). In general, large recharge forces
 230 groundwater to flow deeper than small recharge. As a result, areas with larger
 231 recharge tend to have younger groundwater at the same depth. The variation in the
 232 groundwater age weakens with depth because of the effect of the bottom boundary.
 233 This negative correlation between R_m and the groundwater age attenuates with
 234 distance downgradient due to the cumulative effect of the spatial recharge.

235



236

237 **Figure 4** Selected distribution of simulated groundwater age with R_m in sinusoidal
 238 patterns shown in Equation 2: (a) – (d): specified R_m parameters with same B at 2000

239 mm/y, but A at 12.5, 25, 35 and 50 mm/y, respectively; (e) – (h): specified R_m
240 parameters with same A at 25 mm/y, but B at 500, 1000, 2000 and 5000 mm/y,
241 respectively. (g) is the same as (b).

242

243 The variability in the groundwater age distribution correlates well with the variability
244 in R_m . As the amplitude of the sinusoidal recharge increases, the groundwater age
245 fluctuates more strongly at the same location on the left side of the aquifer domain
246 (Figure 4a to Figure 4d). As groundwater age is controlled by groundwater
247 hydrodynamics, the age fluctuation weakens laterally (the amplitudes of the age
248 isolines decrease from left to right). The change in the age distribution is more evident
249 with the increase in B (Figure 4e to Figure 4g). Larger wavelength results in weaker
250 variation in the age on the left of the domain but stronger variation on the right.

251

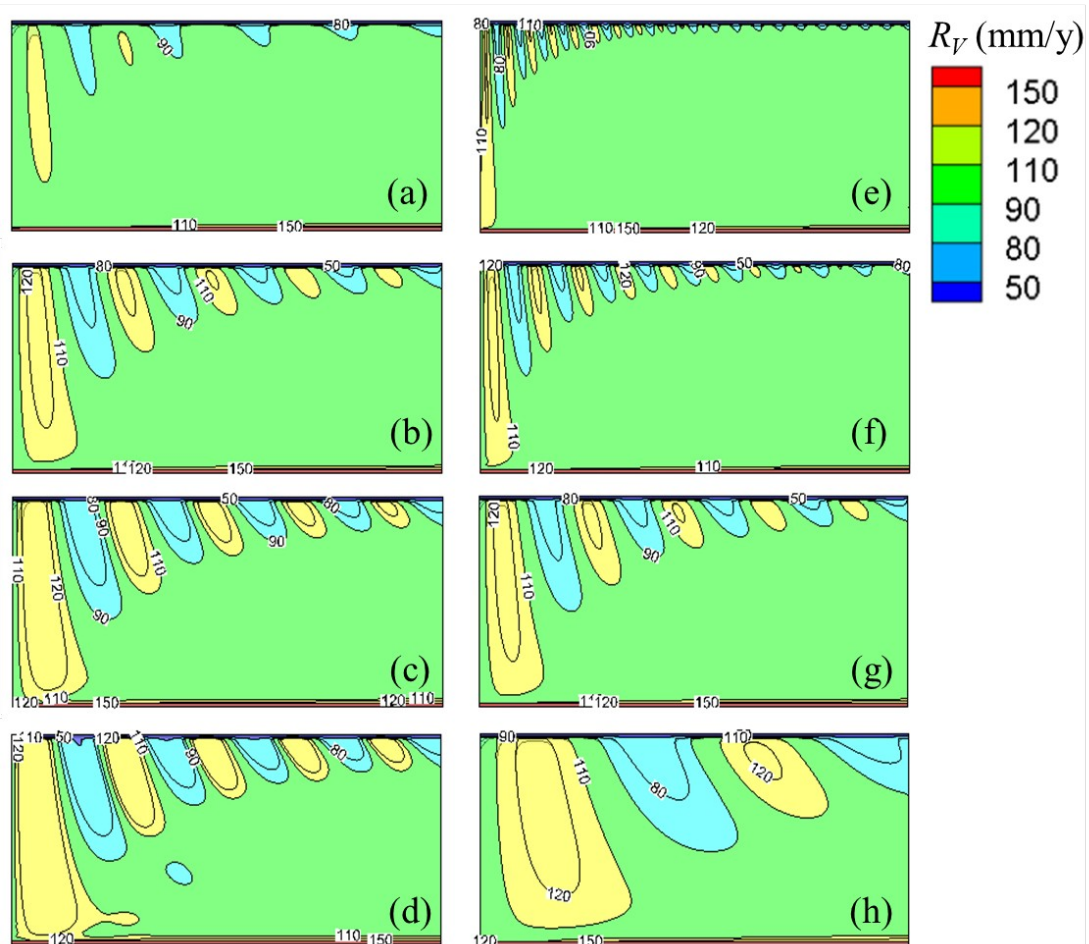
252 We then calculated R_V with the analytical method shown in Equation (1). At the lateral
253 direction, the estimated recharge is strongly variable close to the land surface and
254 becomes relatively stable deeper in the aquifer (Figure 5). Most of the estimated
255 recharge falls in the range of 90–110 mm/y. The recharge close to the left boundary is
256 more likely to deviate from the mean recharge (100 mm/y).

257

258 The variation in the groundwater recharge amplitude and wavelength strongly affects
259 the groundwater recharge estimation. It can be seen that R_V at a certain depth (e.g., Z
260 = 25 m, close to the bottom) becomes more variable as the amplitude increases. The

261 wavelength of R_V also changes in response to the change in the groundwater
 262 wavelength. The probability of overestimating or underestimating recharge rates
 263 increases with both the amplitude and the wavelength increase.

264



265

266 **Figure 5** Selected R_V distribution using simulated groundwater age (shown in Figure
 267 4) and Equation 1: (a) – (d): specified R_m parameters with same B at 2000 mm/y, but
 268 A at 12.5, 25, 35 and 50 mm/y, respectively; (e) – (h): specified R_m parameters with
 269 same A at 25 mm/y, but B at 500, 1000, 2000 and 5000 mm/y, respectively. (g) is the
 270 same as (b). It should be emphasized that the R_V distribution indicates potential
 271 groundwater recharge for the top surface.

272

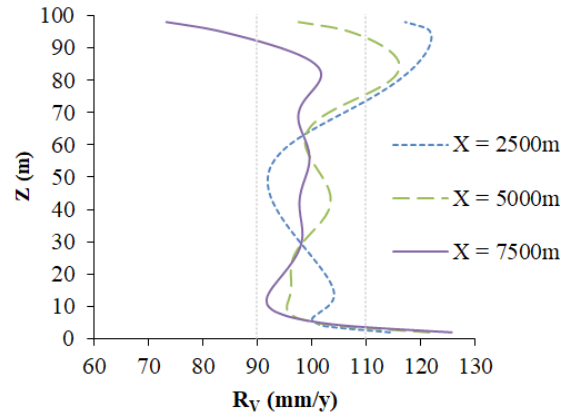
273 **3.3 Estimating long-term average recharge**

274 As shown in Figure 6, R_V varies with depth. At the shallow part of the aquifer, R_V
275 could strongly deviate from the mean R_m . But this R_V would be more representative of
276 local recharge because of limited mixing of local water with regional groundwater
277 passing by. Depending on the location of a sampling well, R_V near the water table
278 could be lower or greater than the mean R_V .

279

280 In addition, Figure 6 suggests that R_V would generally be greater than the mean R_m
281 closer to the bottom boundary regardless of locations. This is because the bottom
282 boundary restricted groundwater from flowing deeper down and so horizontal flow
283 component becomes greater closer to the bottom boundary. This boundary effect
284 results in younger groundwater age and therefore larger groundwater recharge.
285 Despite different degrees of variability in R_V at different sampling well locations, All
286 the mean R_V values estimated from these three locations fall in the accepted mean
287 recharge range (103.9, 103.2 and 97.1 mm/y for $X = 2500, 5000$ and 7500 m,
288 respectively).

289



290

291 **Figure 6** Comparison of estimated recharge for the case with $A = 25$ mm/y and $B =$
 292 2000 m at individual sampling well locations. Numbers shown on the legend indicate
 293 the distance from the model left boundary. Grey lines show the upper and lower
 294 bounds of the acceptable recharge range.

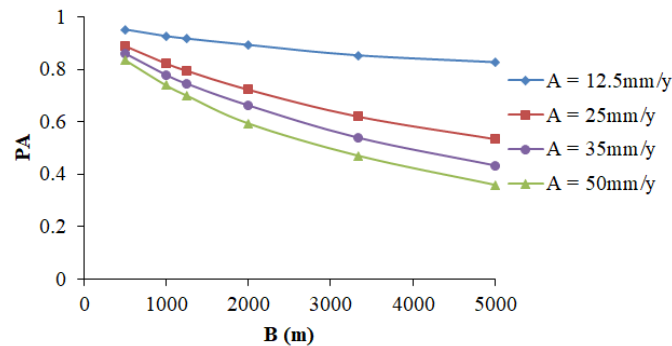
295

296 Recharge estimates are known to be uncertain. If 10% error is assumed in the mean
 297 recharge in our case, then R_V will be reasonable if it falls in the range of 90–110 mm/y
 298 (see grey bounds in Figure 6). We can obtain reasonable recharge estimates from all
 299 the sites if sampling is conducted within a reasonable sampling depth far from both
 300 the water table and the bottom boundary (e.g., $Z = 25$ – 75 m in our case). R_V still
 301 fluctuates vertically but all the values are located between the uncertainty bounds of
 302 the actual recharge. Of course, R_V variability becomes weaker further downgradient if
 303 the sampling activity occurs at downstream locations (Compare the profile of $X =$
 304 7500 m to the other two profiles in Figure 6).

305

306 We can calculate the percentage of area (PA) that may yield acceptable recharge

307 between 90 and 110 mm/y (green area in Figure 5). As seen in Figure 7, as high as
 308 95% of the aquifer domain can provide the recharge in the acceptable range. PA
 309 generally decreases with the increase in A and also B. When A is small (12.5 mm/y),
 310 the estimated recharge does not change significantly with the increase in B (the lowest
 311 PA is 89% for A at 5000 m). However, dramatic change can be observed for the other
 312 A values. Only 36% of the aquifer domain can result in the recharge within the
 313 reasonable range for the worst scenario.



314

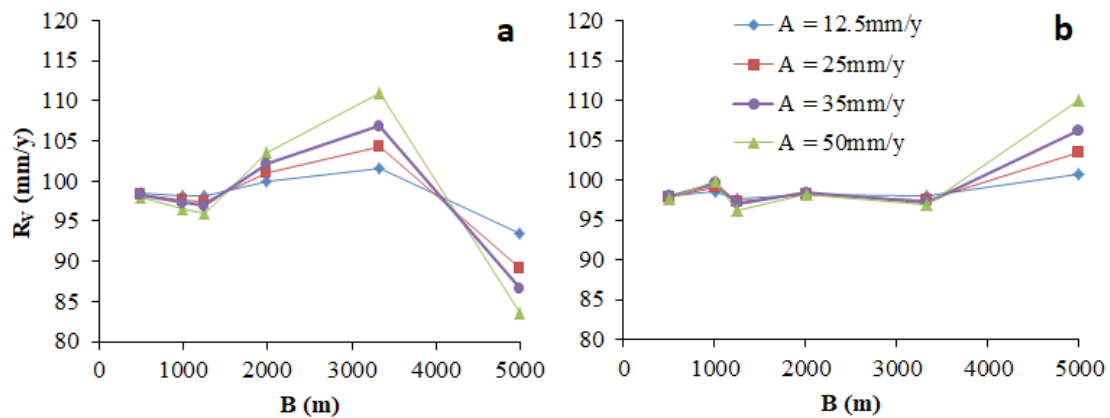
315 **Figure 7** Variation in the percentage of area (PA) with wavelength (B) for different
 316 amplitudes (A). Each PA was calculated by deriving the area with mean recharge
 317 between 90 and 110 mm/y first and then dividing this area by the domain area. A
 318 higher PA indicates a greater chance of obtaining true mean recharge.

319

320 Several depths can be sampled to obtain multiple recharge rates to compute mean R_V .
 321 The mean R_V in Figure 6 would be 101.0, 102.1 and 98.0 mm/y if we used samples
 322 from three depths at $Z = 25, 50$ and 75 m. We computed the mean R_V for all the other
 323 cases. At the location of $X = 5000$ m (Figure 8a), most mean R_V values are located
 324 between 90 and 110 mm/y, except when B is 5000 m. All the mean R_V values are

325 within the acceptable range at the location of $X = 7500$ m (Figure 8b). In comparison
 326 to Figure 7, there is no clear trend in the mean R_V with the change in A or B. This is
 327 because groundwater age patterns are highly dependent on the forcing at the top
 328 boundary. A fixed sampling site could be located at either low or high values of the
 329 boundary forcing. Overall, it is more likely to obtain reasonable mean R_V if we use
 330 multiple depths and place a sampling well at a downstream site.

331



332

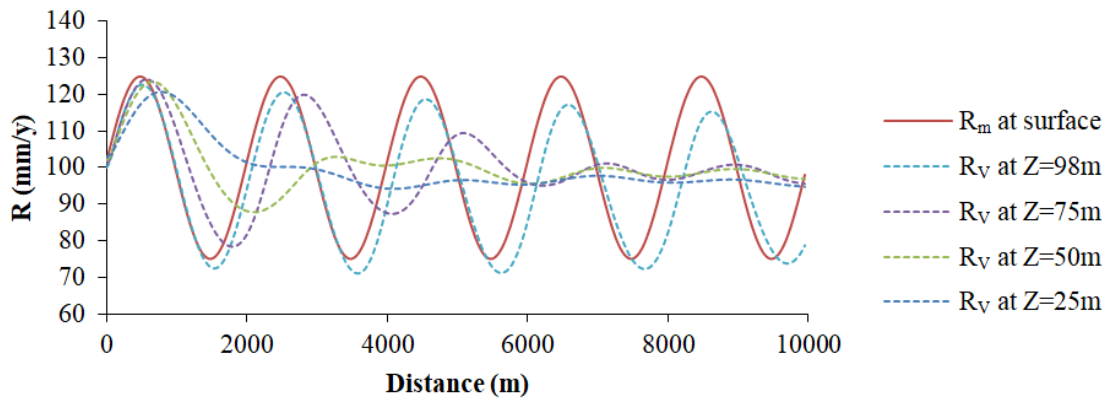
333 **Figure 8** Mean recharge at the depth range of 25–75 m at (a) $X = 5000$ m; (b) $X =$
 334 7500 m

335 3.4 Estimating spatially-varying recharge

336 Figure 9 compares the recharge estimated from the Vogel method for different depths.
 337 As R_m varies in a sinusoidal manner, R_V also varies periodically with distance but its
 338 amplitude diminishes with the increase in the number of recharge cycles. It can be
 339 seen that the Vogel method slightly underestimate the recharge pattern when using the
 340 groundwater age at 98 m from the bottom (2 m beneath the water table) but overall
 341 the performance is reasonable in obtaining spatial R_V . When the groundwater age at 25

342 to 75 m is used, the Vogel method works better for estimating spatial R_V on the left-
 343 hand and mean R_V on the right-hand side of the model.

344



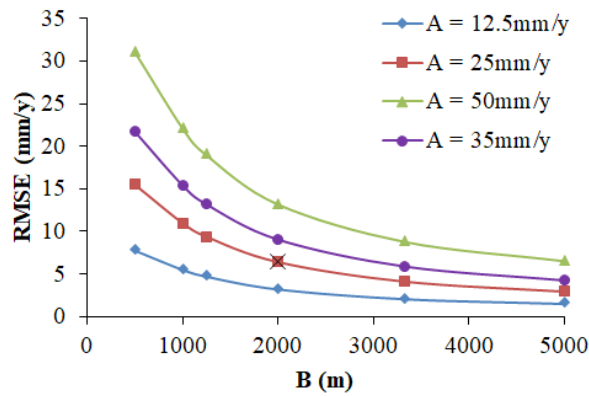
345

346 **Figure 9** Comparison of estimated recharge (R_V) to modeled recharge (R_m) for the
 347 case with $A = 25$ mm/y and $B = 2000$ m at different depths. Numbers shown on the
 348 legend indicate the distance from the model bottom. Root mean squared error
 349 (RMSE) between R_V and R_m is 18.2, 18.1, 17.9 and 8.1 mm/y for 25 m, 50 m, 75 m
 350 and 98 m from the bottom, respectively.

351

352 The spatial variation in R_V may be estimated reasonably for small magnitudes and
 353 large wavelengths, particularly for large wavelengths ($B = 5000$ m in Figure 10). This
 354 condition generally occurs in fluvial plains with less variation in terrain topography.
 355 The ability of the method to estimate spatially-varying R_V becomes worse as the
 356 variable A increases and B decreases. This is mostly because larger variation in R_m
 357 causes stronger hydrodynamic mixing. Hence, it is difficult to estimate spatial R_V in
 358 mountainous regions with the Vogel method.

359



360

361 **Figure 10** Root mean squared error (RMSE) between spatial R_m and spatial R_V using
 362 groundwater age at $Z = 98$ m (2 m below the water table) under different variability
 363 conditions. The black cross represents RMSE between the curves of R_m and R_V at $Z =$
 364 98m in Figure 9.

365

366 It needs to be noted that we also conducted other scenarios with different mean
 367 recharge values (150 mm/y and 50 mm/y). The modeling shows similar trends in the
 368 changes of age, R_V distributions and RMSE between spatial R_m and spatial R_V
 369 presented above due to similar variation in R_m (not shown).

370

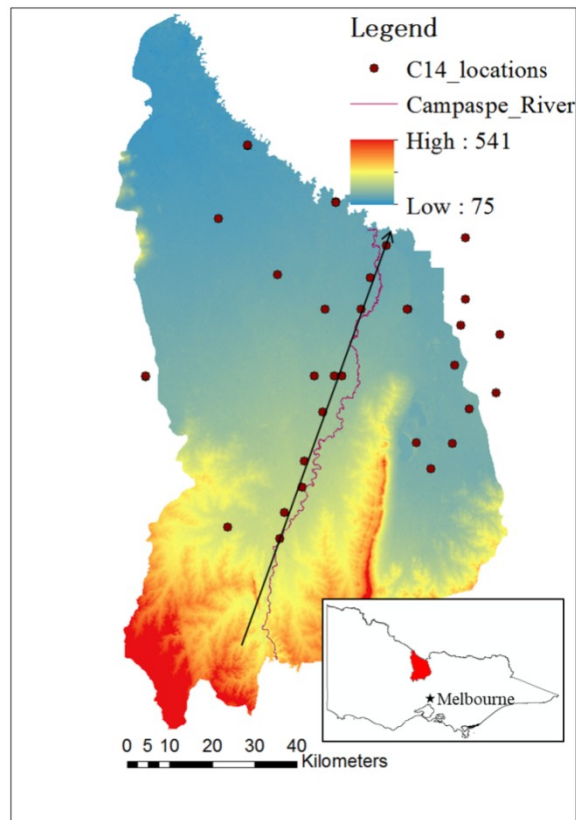
371 4. Field example

372 4.1 Field site and data description

373 Lower Campaspe catchment in southeast Australia was employed to demonstrate the
 374 variation in recharge rates (Figure 11). The entire catchment covers an area of 7,949
 375 km² and forms part of the Murray-Darling Basin. The southern edge of the catchment
 376 is the Great Dividing Range (not shown in the map) and the lower part belongs to the

377 floodplains of the Campaspe and Murray rivers. Soils in this area are generally
378 Sodosols and Vodosols with varying thicknesses according to the Australian Soil
379 Classification system. The aquifers are composed of a shallow unconfined aquifer
380 with interbedded sand and clay and a deep semi-confined aquifer consisting of coarse
381 sand. The water table is usually 10–15 m below the land surface. Long-term annual
382 mean rainfall is around 400 mm/y in the north, whereas long-term annual mean
383 potential evapotranspiration is 1700 mm/y.

384

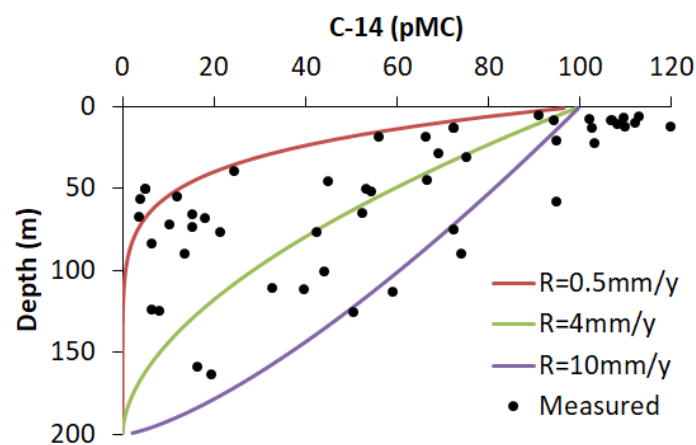


385

386 **Figure 11** Location of the study area and groundwater ^{14}C sampling sites. The black
387 arrow indicates the cross-section where C-14 data were examined.

388

389 Dozens of Carbon-14 (^{14}C) samples were collected over the past years, including
 390 those published in previous studies (Cartwright, 2010) and those collected afterwards
 391 but not published. These data scattered in the lower Campaspe catchment, mostly
 392 along the river or close to the northern boundary. The screen depths of the bores
 393 where ^{14}C samples were taken were lower than 20 m below the ground surface and the
 394 screen lengths were smaller than 10% of the screen depth. ^{14}C was used to understand
 395 groundwater residence times and therefore help conceptualize the groundwater flow
 396 system which is critical for groundwater resource management. As shown in Figure
 397 12, some bores have ^{14}C activities greater than 100 pMC. This indicates that the
 398 groundwater around these bores was recharged after nuclear weapon tests in the 1950s
 399 to 1960s. However, this recharge process occurs usually in the shallow part of the
 400 aquifer, mostly likely in areas that have shallow water table. ^{14}C values in most bores
 401 are usually lower than 100 pMC. There is a general negative correlation between ^{14}C
 402 activity and groundwater depth.



403
 404 **Figure 12** Relationship between ^{14}C and groundwater depth. Black dots are measured
 405 ^{14}C , whereas curves show ideal relationship for different recharge rates calculated

406 with Equation 1 and the ^{14}C decay formula.

407

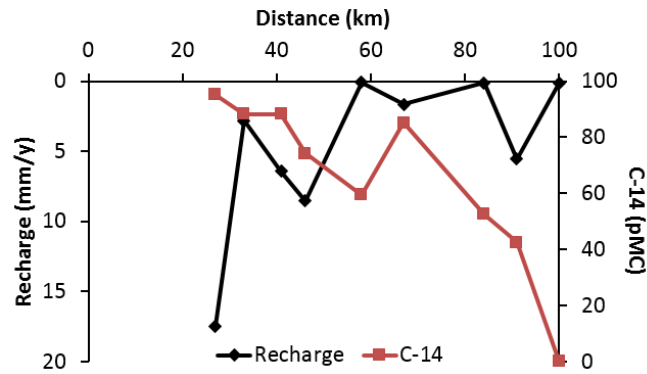
408 **4.2 Groundwater recharge estimates**

409 All the data could be used to estimate long-term average recharge over the entire
410 catchment. We first assumed certain recharge rates and back calculated groundwater
411 age with Equation (1). We then inferred ^{14}C activities from the radioactive decay
412 formula where the half life is 5730 years. The theoretical relationship between ^{14}C and
413 depth is shown in Figure 12 for different recharge scenarios. We can see that the
414 average recharge may range from 0.5 mm/y to 10 mm/y. This recharge represents
415 long-term average recharge over the entire area. Of course, some data are still outside
416 of the ^{14}C -depth curves for lower and upper recharge bounds. These data may indicate
417 smaller or larger recharge rates in some parts of the catchment.

418

419 Individual ^{14}C data can be used to estimate recharge spatially. It can be seen that
420 recharge rates are generally larger in the south of the catchment but become lower
421 towards the north (Figure 13). According to our theoretical analysis in Section 3, the
422 data in the northern part are more representative of larger-scale recharge rates. Hence,
423 if we have only limited data, it is best to make use of data located in the downgradient
424 area. This finding is consistent with the recharge bounds identified from all the data
425 above.

426



427

428 **Figure 13** Groundwater ^{14}C data and recharge rates versus distance from the
 429 designated starting point along a transect shown in Figure 11.

430

431 Our theoretical analysis also indicates that combined use of tracers at different depths
 432 could be used to obtain recharge representative of larger areas. It is not very common
 433 to have ^{14}C data at different depths in one bore. This is also the case in our field site.
 434 However, if we could combine tracer data close to the downstream (e.g., the three
 435 sites close to the 100 km), we would obtain the average recharge rate of 1.9 mm/y.
 436 This recharge estimate is still within the range identified in Figure 12. However,
 437 according to our theoretical analysis, this recharge estimate may be more
 438 representative of true recharge rates, although it is still very subjective.

439

440 5. Discussion

441 This study examined the validity of the popular Vogel method to quantify mean
 442 groundwater recharge and the possibility of using this method to estimate recharge
 443 reliably. Several numerical experiments were performed to simulate groundwater age
 444 distribution under different boundary conditions and one field example was provided.

445

446 5.1 Estimation of long-term average groundwater recharge

447 Our study showed that groundwater age determined from certain part of an aquifer
448 can be used to infer long-term average groundwater recharge through the Vogel
449 method (Vogel, 1967) under spatially-varying conditions. This ability of the Vogel
450 method to estimate long-term average recharge is because age tracers are largely
451 driven by advection and dispersion which is related to hydraulic forcing at the top
452 surface (Sanford, 2010). Of course, as actual recharge is usually spatially varying
453 (McMahon, Plummer, Böhlke, Shapiro, & Hinkle, 2011), estimated recharge will be
454 closer to the actual long-term average value if samples are collected from a
455 downgradient monitoring well and at a relatively large depth.

456

457 Our study indicates that long-term average groundwater recharge could be estimated
458 reasonably if groundwater age samples are collected properly. However, it is often
459 hardly possible to ascertain whether groundwater wells are placed in proper places, as
460 groundwater age is strongly influenced by groundwater hydrodynamics and
461 dispersion effects (McMahon, Plummer, Böhlke, Shapiro, & Hinkle, 2011). Therefore,
462 any samples could be biased from the actual recharge like many existing studies (e.g.,
463 Hinkle, Böhlke, Duff, Morgan, & Weick, 2007; Harrington, Cook, & Herczeg, 2002;
464 Hagedorn, El-Kadi, Mair, Whittier, & Ha, 2011; McMahon, Plummer, Böhlke,
465 Shapiro, & Hinkle, 2011). Hence, combining recharge estimates from multiple depths
466 would yield more reliable long-term average recharge estimates (Harrington, Cook, &

467 Herczeg, 2002). This is particularly true if our sampling sites are located upgradient
468 where estimated recharge may vary strongly with depth (see Figure 6). In reality,
469 many groundwater wells are determined beforehand and probably with long screens
470 for water supply purposes. These wells could also be utilized for estimating long-term
471 average recharge if the entire screens are located within the unconfined aquifer,
472 because groundwater from different depths will mix completely during sampling.

473

474 **5.2 Spatial groundwater recharge estimation**

475 Actual groundwater recharge is known to vary in space and time. Many efforts have
476 been made to derive spatial groundwater recharge (e.g., Crosbie, McCallum, Walker,
477 & Chiew, 2010; Harrington, Cook, & Herczeg, 2002; Keese, Scanlon, & Reedy, 2005;
478 Nolan, Baehr, & Kauffman, 2003; Xie, Crosbie, Simmons, Cook, & Zhang, 2019).
479 Most methods make use of unsaturated zones as they are easily accessible and cost is
480 relatively low (Keese, Scanlon, & Reedy, 2005; Nolan, Baehr, & Kauffman, 2003;
481 Xie, Crosbie, Simmons, Cook, & Zhang, 2019). While they reflect on the variation in
482 spatial groundwater recharge, the results are in fact potential groundwater recharge.
483 Whether potential recharge is equal to actual recharge is dependent on a number of
484 factors including thickness of unsaturated zones, degree of soil heterogeneity, and
485 moisture content of underlying soil layers. Our study proposes that the Vogel method
486 can also be used to estimate spatially varying actual recharge directly without the need
487 to consider the factors mentioned above. What is required is to reliably determine

488 groundwater age close to the water table. Although this method may be theoretically
489 better than the soil water balance method, it is much more expensive to obtain a
490 sufficient number of groundwater age samples for the same purpose. Therefore,
491 combinations of field methods including groundwater age method, soil water balance,
492 chloride mass balance and tritium profile method are encouraged (e.g., Healy, 2010;
493 Scanlon, Healy, & Cook, 2002).

494

495 This study assumed that groundwater age at the water table is zero. This assumption is
496 appropriate in humid regions where water table is shallow. Infiltrating water can reach
497 the water table within a short time. However, this assumption is not always valid in
498 arid and semiarid regions. In thick arid unsaturated zones it can take hundreds and
499 even up to thousands of years for infiltrating water to reach the water table (Cook,
500 Edmunds, & Gaye, 1992; Love et al., 2013; Wood, Cook, & Harrington, 2015).
501 Therefore, under these conditions when estimating recharge in arid and semiarid
502 regions, groundwater age above the water table must also be known in priori.

503

504 **5.3 Limitations**

505 Our study suggests that both long-term average and spatially varying groundwater
506 recharge could be estimated with the Vogel method under spatially varying conditions.

507 Our study represents a further step towards better quantifying groundwater recharge
508 with existing methods. We built our study on the simple homogeneous and isotropic
509 aquifer conceptualization to examine the potential impact of complex boundary

510 conditions on groundwater recharge estimation. We are acutely aware that aquifer
511 heterogeneity may significant affect flow fields and therefore recharge estimation as
512 shown by Kozuskanich, Simmons, & Cook (2014). Given that numerous existing
513 studies assume homogeneous settings (e.g., Hinkle, Böhlke, Duff, Morgan, & Weick,
514 2007; Harrington, Cook, & Herczeg, 2002; Hagedorn, El-Kadi, Mair, Whittier, & Ha,
515 2011) and our main objective was not on assessing the impact of aquifer
516 heterogeneity, we based our model on those existing studies with homogeneous
517 conceptualization.

518

519 In addition, actual groundwater recharge is variant both in space and time. As the
520 Vogel method assumes a steady state setting, this study did not consider temporal
521 changes in recharge. Temporal variation in recharge are best examined through
522 numerical modeling which has been frequently studied (e.g., Xie, Crosbie, Simmons,
523 Cook, & Zhang, 2019). Dispersive mixing is another factor that may contribute to the
524 complexity in estimating recharge with this method, but it is beyond the scope of our
525 study. Greater dispersivity causes stronger mixing in water particles and decay
526 isotopes and likely results in a younger age and a greater recharge rate. This impact of
527 dispersion needs be studied in a future study.

528

529 **6. Conclusions**

530 This study performed several numerical experiments in order to examine the validity

531 of the simplified analytical method to estimate spatial recharge. We first generated
532 different flow fields and age patterns with different spatially-varying fluxes as model
533 upper boundary conditions. We then estimated groundwater recharge using the
534 analytical method at the spatial scale and examined the differences between analytical
535 and modelled recharge rates. A field example was provided in the end to illustrate our
536 results as much as possible. Several remarks can be made based on this study.

537 Long-term average groundwater recharge can be estimated reasonably well provided
538 that the age sample is collected from the middle of an aquifer and at downstream
539 areas. Multiple groundwater age measurements can be averaged to improve the
540 precision of the long-term average groundwater recharge. This simple analytical
541 method can also be used to estimate local groundwater recharge if age samples are
542 collected below the water table.

543

544 **Acknowledgements**

545 The research is financially supported by the Science Foundation of Key Laboratory of
546 Shale Gas and Geoengineering, Institute of Geology and Geophysics, Chinese
547 Academy of Sciences (No. KLSG201704), Hydrogeological Investigation at 1:50 000
548 Scale in the Kongque River Catchment of Tarim Basin (DD20190351), the National
549 Natural Science Foundation of China (41402226) and by Key Laboratory for
550 Groundwater and Ecology in Arid and Semi-Arid Areas, Xi'an Center of China
551 Geological Survey (No. KLGEAS201601).The authors thank the anonymous
552 reviewers for their constructive suggestions.

553 Conflicts of Interest

554 The authors declare no conflict of interest.

555

556 Data Availability

557 Data used in this study can be provided by the corresponding author upon request.

558

559 References

560 Aquanty Inc. (2018). HydroGeoSphere. A three-dimensional numerical model
561 describing fully-integrated subsurface and surface flow and solute transport.

562 Waterloo, Ontario, Canada. <https://www.aquanty.com/hgs-download>

563 Allison, G. B., Gee, G. W., & Tyler, S. W. (1994). Vadose-zone techniques for
564 estimating groundwater recharge in arid and semiarid regions. *Soil Science*

565 *Society of America Journal*, 58, 6-14. [https://doi.org/](https://doi.org/10.2136/sssaj1994.03615995005800010002x)

566 10.2136/sssaj1994.03615995005800010002x

567 Cartwright, I. (2010). Using groundwater geochemistry and environmental isotopes to
568 assess the correction of ^{14}C ages in a silicate-dominated aquifer system. *Journal*

569 *of Hydrology*, 382, 174–187. <https://doi.org/10.1016/j.jhydrol.2009.12.032>

570 Chesnaux, R., Molson, J. W., & Chapuis, R. P. (2005). An analytical solution for
571 ground water transit time through unconfined aquifers. *Ground Water*, 43, 511-

572 517. <https://doi.org/10.1111/j.1745-6584.2005.0056.x>

573 Chesnaux, R., Santoni, S., Garel, E., & Huneau, F. (2018). An analytical method for

574 assessing recharge using groundwater travel time in Dupuit flow aquifers.

- 575 *Ground Water*, 56, 986-992. <https://doi.org/10.1111/gwat.12794>
- 576 Cook, P. G., & Böhlke, J. K. (2000). Determining timescales for groundwater flow
577 and solute transport. In P. G. Cook & A. L. Herczeg (Eds.), *Environmental*
578 *tracers in subsurface hydrology* (pp. 1-30). Boston: Kluwer Academic Publisher.
- 579 Cook, P. G., Edmunds, W. M., & Gaye, C. B. (1992). Estimating paleorecharge and
580 paleoclimate from unsaturated zone profiles. *Water Resources Research*, 28,
581 2721-2731. <https://doi.org/10.1029/92WR01298>
- 582 Cook, P. G., Walk, G. R., & Jolly, I. D. (1989). Spatial variability of groundwater
583 recharge in a semiarid region. *Journal of Hydrology*, 111, 195-212.
584 [https://doi.org/10.1016/0022-1694\(89\)90260-6](https://doi.org/10.1016/0022-1694(89)90260-6)
- 585 Crosbie, R. S., McCallum, J. L., Walker, G. R., & Chiew, F. H. S. (2010). Modelling
586 climate-change impacts on groundwater recharge in the Murray-Darling Basin,
587 Australia. *Hydrogeology Journal*, 18, 1639-1656. [https://doi.org/](https://doi.org/10.1007/s10040-010-0625-x)
588 [10.1007/s10040-010-0625-x](https://doi.org/10.1007/s10040-010-0625-x)
- 589 de Vries, J. J., & Simmers, I. (2002). Groundwater recharge: An overview of
590 processes and challenges. *Hydrogeology Journal*, 10, 5-17. [https://doi.org/](https://doi.org/10.1007/s10040-001-0171-7)
591 [10.1007/s10040-001-0171-7](https://doi.org/10.1007/s10040-001-0171-7)
- 592 Goode, D. J. (1996). Direct simulation of groundwater age. *Water Resources*
593 *Research*, 32, 289-296. <https://doi.org/10.1029/95WR03401>
- 594 Healy, R. W. (2010). *Estimating Groundwater Recharge*. Cambridge University Press.
- 595 Hinkle, S. R., Böhlke, J. K., Duff, J. H., Morgan, D. S., & Weick, R. J. (2007).
596 Aquifer-scale controls on the distribution of nitrate and ammonium in ground

- 597 water near La Pine, Oregon, USA. *Journal of Hydrology*, 333, 486-503.
598 <https://doi.org/10.1016/j.jhydrol.2006.09.013>
- 599 Harrington, G. A., Cook, P. G., & Herczeg, A. L. (2002). Spatial and temporal
600 variability of ground water recharge in central Australia: A tracer approach.
601 *Ground Water*, 40, 518-527. <https://doi.org/10.1111/j.1745-6584.2002.tb02536.x>
- 602 Hagedorn, B., El-Kadi, A. I., Mair, A., Whittier, R. B., & Ha, K. (2011). Estimating
603 recharge in fractured aquifers of a temperate humid to semiarid volcanic island
604 (Jeju, Korea) from water table fluctuations, and Cl, CFC-12 and ³H chemistry.
605 *Journal of Hydrology*, 409, 650-662. [https://doi.org/](https://doi.org/10.1016/j.jhydrol.2011.08.060)
606 [10.1016/j.jhydrol.2011.08.060](https://doi.org/10.1016/j.jhydrol.2011.08.060)
- 607 Kim, J. H., & Jackson, R. B. (2012). A global analysis of groundwater recharge for
608 vegetation, climate, and soils. *Vadose Zone Journal*, 11. [https://doi.org/](https://doi.org/10.2136/vzj2011.0021RA)
609 [10.2136/vzj2011.0021RA](https://doi.org/10.2136/vzj2011.0021RA)
- 610 Kozuskanich, J., Simmons, C. T., & Cook, P. G. (2014). Estimating recharge rate from
611 groundwater age using a simplified analytical approach: Applicability and error
612 estimation in heterogeneous porous media. *Journal of Hydrology*, 511, 290-294.
613 <https://doi.org/10.1016/j.jhydrol.2014.01.058>
- 614 Keese, K. E., Scanlon, B. R., & Reedy, R. C. (2005). Assessing controls on diffuse
615 groundwater recharge using unsaturated flow modeling. *Water Resources*
616 *Research*, 41, W06010. <https://doi.org/10.1029/2004WR003841>
- 617 Love, A. J., Shand, P., Karlstrom, K., Crossey, L., Rousseau-Gueutin, P., Priestley,
618 S., ... Keppel, M. (2013). Geochemistry and travertine dating provide new

- 619 insights into the hydrogeology of the Great Artesian Basin, South Australia.
620 *Procedia Earth and Planetary Science*, 7, 521-524.
621 <https://doi.org/10.1016/j.proeps.2013.03.065>
- 622 McMahon, P. B., Bohlke, J. K., & Carney, C. P. (2007). Vertical gradients in water
623 chemistry and age in the northern High Plains Aquifer, Nebraska, 2003. *US Geol.*
624 *Surv. Sci. Invest. Rep.* (pp. 2006-5294).
- 625 McMahon, P. B., Plummer, L. N., Böhlke, J. K., Shapiro, S. D., & Hinkle, S. R.
626 (2011). A comparison of recharge rates in aquifers of the United States based on
627 groundwater-age data. *Hydrogeology Journal*, 19, 779-800.
628 <https://doi.org/10.1007/s10040-011-0722-5>
- 629 Nolan, B. T., Baehr, A. L., & Kauffman, L. J. (2003). Spatial variability of
630 groundwater recharge and its effect on shallow groundwater quality in southern
631 New Jersey. *Vadose Zone Journal*, 2, 677-691.
- 632 Priestley, S., Shand, P., Love, A., Crossey, L., & Karlstrom, K. (2013). Groundwater
633 recharge, hydrodynamics and hydrochemistry of the western Great Artesian
634 Basin. In A. J. Love, D. Wohling, S. Fulton, P. Rousseau-Gueutin, & S. De Ritter
635 (Eds.), *Allocating water and maintaining springs in the Great Artesian Basin* (pp.
636 171-201). Canberra, Australia: Natl Water Community.
- 637 Sanford, W. (2002). Recharge and groundwater models: An overview. *Hydrogeology*
638 *Journal*, 10, 110-120. <https://doi.org/10.1007/s10040-001-0173-5>
- 639 Sanford, W. (2010). Coastal flow. *Nature Geoscience*, 3, 671-672.
640 <https://doi.org/10.1038/ngeo958>

- 641 Scanlon, B. R., Healy, R. W., & Cook, P. G. (2002). Choosing appropriate techniques
642 for quantifying groundwater recharge. *Hydrogeology Journal*, *10*, 18-39.
643 <https://doi.org/10.1007/s10040-011-0722-5>
644 Scanlon, B. R., Keese, K. E., Flint, A. L., Flint, L. E., Gaye, C. B., Edmunds, W. M.,
645 & Simmers, I. (2006). Global synthesis of groundwater recharge in semiarid and
646 arid regions. *Hydrological Processes*, *20*, 3335-3370.
647 <https://doi.org/10.1002/hyp.6335>
- 648 Vogel, J. C. (1967). Investigation of groundwater flow with radiocarbon. In *Isotopes*
649 *in Hydrology* (pp. 355-369). Vienna: IAEA.
- 650 Wood, C., Cook, P. G., & Harrington, G. A. (2015). Vertical carbon-14 profiles for
651 resolving spatial variability in recharge in arid environments. *Journal of*
652 *Hydrology*, *520*, 134-142. <https://doi.org/10.1016/j.jhydrol.2014.11.044>
- 653 Xie, Y., Crosbie, R., Simmons, C. T., Cook, P. G., & Zhang, L. (2019). Uncertainty
654 assessment of spatial-scale groundwater recharge estimated from unsaturated
655 flow modelling. *Hydrogeology Journal*, *27*, 379-393.
656 <https://doi.org/10.1007/s10040-018-1840-0>
- 657 Xie, Y., Cook, P. G., Shanafield, M., Simmons, C. T., & Zheng, C. (2016). Uncertainty
658 of natural tracer methods for quantifying river-aquifer interaction in a large river.
659 *Journal of Hydrology*, *535*, 135-147. [https://doi.org/](https://doi.org/10.1016/j.jhydrol.2016.01.071)
660 [10.1016/j.jhydrol.2016.01.071](https://doi.org/10.1016/j.jhydrol.2016.01.071)
- 661 Xie, Y., Crosbie, R., Yang, J., Wu, J., & Wang, W. (2018). Usefulness of soil moisture
662 and actual evapotranspiration data for constraining potential groundwater

663 recharge in semiarid regions. *Water Resources Research*, 54, 4929-4945.

664 <https://doi.org/10.1029/2018WR023257>

665 Yang, Y., Wang, Z., Xie, Y., Ataie-Ashtiani, B., Simmons, C. T., Luo, Q., ... Wu, J.

666 (2019). Impacts of groundwater depth on regional scale soil gleyization under

667 changing climate in the Poyang Lake Basin, China. *Journal of Hydrology*, 568,

668 501-516. <https://doi.org/10.1016/j.jhydrol.2018.11.006>